



Geomorphology of Ulu Peninsula, James Ross Island, Antarctica

Stephen J. A. Jennings ^a, Bethan J. Davies ^b, Daniel Nývlt ^{a,c}, Neil F. Glasser ^d, Zbyněk Engel ^e, Filip Hrbáček ^a, Jonathan L. Carrivick ^f, Bedřich Mlčoch ^c and Michael J. Hambrey ^d

^aPolar-Geo-Lab, Department of Geography, Faculty of Science, Masaryk University, Brno, Czech Republic; ^bCentre for Quaternary Research, Department of Geography, Royal Holloway University of London, Egham, UK; ^cCzech Geological Survey, Praha, Czech Republic; ^dCentre for Glaciology, Department of Geography and Earth Sciences, Aberystwyth University, Wales, UK; ^eDepartment of Physical Geography and Geoecology, Faculty of Science, Charles University, Praha, Czech Republic; ^fSchool of Geography, University of Leeds, Leeds, UK

ABSTRACT

This study presents a 1:25,000 geomorphological map of the northern sector of Ulu Peninsula, James Ross Island, Antarctic Peninsula. The map covers an area of c. 250 km², and documents the landforms and surficial sediments of one of the largest ice-free areas in Antarctica, based on remote sensing and field-based mapping. The large-scale landscape features are determined by the underlying Cretaceous sedimentary and Neogene volcanic geology, which has been sculpted by overlying ice masses during glacial periods. Paraglacial and periglacial features are superimposed upon remnant glacial features, reflecting the post-glacial evolution of the landscape. The study area can be broadly separated into three geomorphological sectors, according to the dominant contemporary Earth-surface processes; specifically, a glacierised southern sector, a paraglacial-dominated eastern sector, and a periglacial-dominated central/northern sector. This map provides a basis for further interdisciplinary research, and insight into the potential future landscape evolution of other parts of the Antarctic Peninsula as the climate warms.

ARTICLE HISTORY

Received 29 September 2020
Revised 17 February 2021
Accepted 17 February 2021

KEYWORDS

Geomorphology;
palaeogeology; Ulu
Peninsula; James Ross Island;
Antarctic Peninsula;
Antarctica

1. Introduction

Prior to the beginning of the twenty-first century, the Antarctic Peninsula was one of the most rapidly warming parts of the World (Carrivick et al., 2012; Oliva et al., 2017; Turner et al., 2005, 2016; Vaughan et al., 2003), with the north-eastern Antarctic Peninsula being particularly susceptible to changes in atmospheric and ocean temperatures (Pritchard et al., 2012). These changes resulted in the acceleration, thinning, and recession of glaciers in the area, as well as the collapse of several large ice shelves (Cook et al., 2005; Cook & Vaughan, 2010; Engel et al., 2012; Glasser et al., 2009; Hodgson, 2011; Pritchard et al., 2012; Seehaus et al., 2018). To improve our understanding of climatic and oceanic forcing in this region there is a need to understand how these dramatic changes fit into longer-term trends and processes. One way to do this is to exploit the geomorphological record to determine past glacier extents, glacier mass balance sensitivities, and controls on ice dynamics. Furthermore, an appreciation of the paraglacial/periglacial evolution of the Antarctic landscape is crucial for assessing how glacierised landscapes across the Antarctic Peninsula will respond to future climate-induced glacial recession and deglaciation (Lee et al., 2017; Siegert et al., 2019).

Geomorphological studies are particularly important in Antarctic landscapes because they can provide information that is difficult to ascertain by other means. For example, the use of marine geological evidence from the continental shelf and terrestrial lacustrine records for establishing ice sheet chronologies in the Antarctic Peninsula region is sometimes problematic because of a large marine reservoir effect that can impede accurate radiocarbon dating (Davies et al., 2012b; Ingólfsson et al., 1992; Pířková et al., 2019; Pudsey et al., 2006), albeit some accurate radiocarbon chronologies have been successfully established (e.g. Charman et al., 2018; Dickens et al., 2019; Sterken et al., 2012; Watcham et al., 2011). Other approaches have relied on cosmogenic nuclide dating techniques or glacial geology investigations for assessing the vertical and dynamic changes in the ice sheet over time. However, in ice-covered areas, these methods are reliant upon the location of nunataks, which can only provide spatially limited, pinpoint data (Balco et al., 2013). Furthermore, the inheritance of cosmogenic isotopes poses a challenge for accurate cosmogenic exposure dating in Antarctica (e.g. Bentley et al., 2006).

The comparatively large expanse of the deglaciated region of the Ulu Peninsula provides an opportunity to study the history of the area on a larger scale than

is possible in other areas of the Antarctic Peninsula, in an area that has been extensively studied (e.g. Glasser et al., 2014; Johnson et al., 2011; Kaplan et al., 2020; Nývlt et al., 2014). By investigating the preserved landforms, the Ulu Peninsula can be treated as a case study for assessing landform evolution in response to future climate change.

The aim of this paper and its associated geomorphological map is to supplement the previously published maps of the Ulu Peninsula (British Antarctic Survey, 2017; Czech Geological Survey, 2009; Davies et al., 2013; Kaplan et al., 2020; Mlčoch et al., 2020; Smellie et al., 2013; Strelin & Malagnino, 1992), as well as other more spatially-limited geomorphological investigations (e.g. Carrivick et al., 2012; Kňázková et al., 2020, 2021; Lundquist et al., 1995; Strelin et al., 2006). This study comprehensively maps the geomorphology of the northern sector of Ulu Peninsula in much greater detail than has previously been achieved, utilising a combination of geological and geomorphological approaches. As the largest deglaciated area in the Antarctic Peninsula region, with c. 250 km² of ice-free terrain mapped in this study, the unprecedented detail and coverage of this study allows the relationships between different landforms to be analysed on a more comprehensive scale, revealing information about past ice dynamics, the history of glacier recession, and paraglacial/periglacial landscape evolution following deglaciation. By providing a comprehensive overview of the geomorphological context of the Ulu Peninsula and its landscape evolution, this study provides a foundation for future multidisciplinary investigations. Furthermore, the geomorphological record may provide insights into the potential landscape evolution of other Antarctic Peninsula regions in response to future climate change.

2. Study area

James Ross Island is situated in the north-western sector of the Weddell Sea, located 7.2 km (at its closest point) off the north-eastern coast of the Antarctic Peninsula (Figure 1) (Ingólfsson et al., 1992). The Ulu Peninsula covers the northernmost part of James Ross Island, located to the north-west of the isthmus separating Röhss Bay and Croft Bay. The majority of ice-free land on James Ross Island (c. 250 km²) is in the northern sector of Ulu Peninsula, extending northward from Whisky Glacier and Shrove Cove (Figure 2). The remaining southern sector of the island is dominated by a large ice cap situated on the now extinct polygenetic shield volcano of Mount Haddington (Smellie, 1999).

The Ulu Peninsula is geologically characterised by soft Cretaceous strata comprising mudstone and

sandstone beds (Crame et al., 1991; Francis et al., 2006; Ineson et al., 1986). These sediments are overlain by multiple horizons of subaqueous/subglacial hyaloclastite breccias and massive subaerial basalts of Neogene age. The volcanic rocks forming the James Ross Island Volcanic Group (Smellie et al., 2008) and host beds of glacial strata are referred to as the Hobbs Glacier Formation at the boundary with Cretaceous strata (Davies et al., 2013; Hambrey et al., 2008; Hambrey & Smellie, 2006; Pirrie et al., 1997), and the Mendel Formation (2011) between individual volcanic sequences. The hyaloclastite and basalt flows form prominent cliffs exposing well-preserved lava-fed deltas (Smellie et al., 2008), and the volcanic rocks form prominent mesa and cinder cone landforms (Davies et al., 2012b; Nehyba & Nývlt, 2014; Nelson et al., 2009; Smellie et al., 2008). Spatially limited outcrops of Neogene to Quaternary unlithified sediments of varying origin are also present overlying the Cretaceous strata (Mlčoch et al., 2020).

It is the geology of the Ulu Peninsula which makes it an ideal location to study the terrestrial record of the dynamics and recession of the Last Glacial Maximum Antarctic Peninsula Ice Sheet because it is distinctly different from that of the nearby Antarctic Peninsula (Glasser et al., 2014; Kaplan et al., 2020; Nývlt et al., 2014). Erratics composed of lithologies that are absent as bedrock on Ulu Peninsula, and therefore must have originated from the mainland Antarctic Peninsula, help to constrain the ice-flow characteristics and deglaciation chronology of the ice sheet by way of cosmogenic exposure dating (e.g. Glasser et al., 2014; Kaplan et al., 2020; Nývlt et al., 2014).

During the Last Glacial Maximum, prior to c. 18 ka, James Ross Island was inundated by the Antarctic Peninsula Ice Sheet, which coalesced with, but did not overrun, the independent Mount Haddington Ice Cap (Bentley & Anderson, 1998; Camerlenghi et al., 2001; Davies et al., 2012b; Evans et al., 2005; Glasser et al., 2014; Heroy & Anderson, 2007; Johnson et al., 2011; Kaplan et al., 2020; Mulvaney et al., 2012; Cofaigh C et al., 2014). However, after c. 18 ka, the ice sheet started to become more dynamic with the development of the Prince Gustav Ice Stream that flowed along the Prince Gustav Channel following regional thinning and increased topographic control (Glasser et al., 2014; Nývlt et al., 2014) (Figures 1 and 2). The formation of this ice stream coincided with a period of rapid eustatic sea-level rise and increasing air temperatures from c. 18–12 ka, with temperatures rising from c. 6.1°C cooler than present at the Last Glacial Maximum to c. 1.3°C warmer than present during the early-Holocene climatic optimum (Hjort et al., 1997; Mulvaney et al., 2012; Roberts et al., 2011). After c. 8 ka, relative sea-level dropped from a maximum of c. 15 m above present as a consequence of rapid isostatic uplift (Roberts et al., 2011), which was

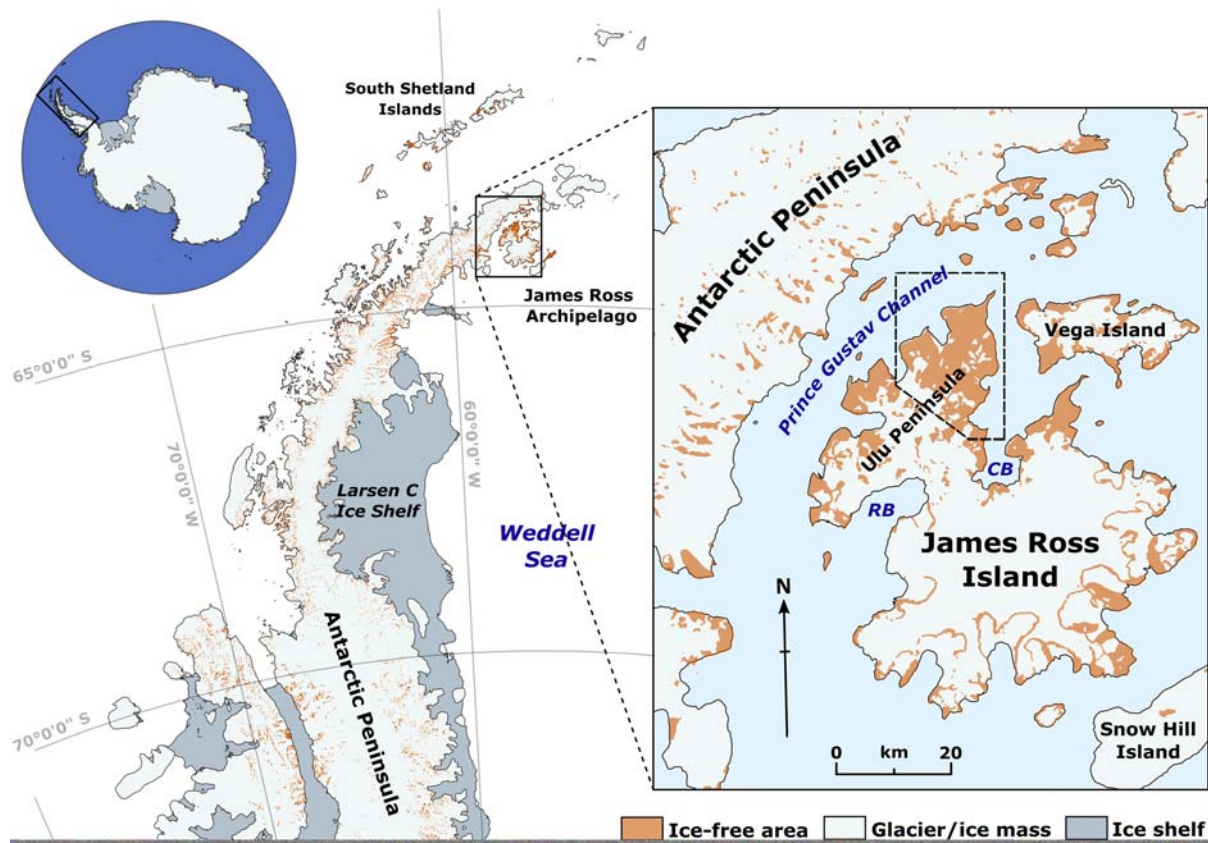


Figure 1. Location map of the study area in relation to the Antarctic Peninsula and James Ross Island. The dashed box located on the inset map of James Ross Island indicates the area covered by the Main map and Figure 2. RB: Röhss Bay; CB: Croft Bay.

concurrent with the deglaciation of the Ulu Peninsula, with ice reaching the approximate present day configuration by c. 6–4 ka (Glasser et al., 2014; Kaplan et al., 2020).

In contrast to the present-day polar maritime climate of the western Antarctic Peninsula, James Ross Island has a semi-arid polar continental climate (Davies et al., 2013; Nývlt et al., 2016; Vaughan et al., 2003). Mean annual air temperatures at sea level in the northern sector of the Ulu Peninsula are around -7°C (Ambrozova et al., 2019), with estimates of precipitation (predominantly falling as snow) ranging from 200 to 500 mm a^{-1} w.e. (water equivalent) (van Lipzig et al., 2004). However, prevailing south to south-westerly winds strongly influence the distribution and drifting of snow (Davies et al., 2013).

Climate records indicate that the Antarctic Peninsula has been warming since the 1930s (Barrand et al., 2013; Vaughan et al., 2003), with ice-core records from the Mount Haddington Ice Cap and lake-core records from Beak Island suggesting a longer period of warming that initiated c. 600 years ago (Mulaney et al., 2012; Sterken et al., 2012). However, recent studies analysing the temperature trend in the Antarctic Peninsula have discovered a shift from a warming trend to a cooling trend since 1998/1999 (Oliva et al., 2017; Turner et al., 2016). These studies indicate that the cooling has been most significant in

the northern and north-eastern sectors of the Antarctic Peninsula, but is absent in the south-western Antarctic Peninsula (Oliva et al., 2017; Turner et al., 2016). The effect of this cooling has already been observed, particularly in the northern to north-eastern tip of the Antarctic Peninsula, where there has been a slow-down of glacier recession, positive mass gains for smaller peripheral glaciers (Engel et al., 2018), and a reduction of permafrost active layer thickness on some islands (Oliva et al., 2017). These changes are strongly influenced by the extent and duration of sea ice cover in the north-western sector of the Weddell Sea and Antarctic Sound (Oliva et al., 2017).

At present, the northern sector of Ulu Peninsula is predominantly ice-free (Figures 1 and 2), with a number of small cirque/valley glaciers and ice domes located on volcanic mesas, or on their slopes (Engel et al., 2012; Glasser et al., 2014; Rabassa et al., 1982). The majority of land-terminating glaciers on Ulu Peninsula are receding (Carrivick et al., 2012; Davies et al., 2012a; Engel et al., 2012; Seehaus et al., 2018), and are surrounded by prominent ice-cored moraines marking c. 100 m of recession since the most recent glacial advance (Carrivick et al., 2012; Davies et al., 2013). Since that advance, glaciers on Ulu Peninsula have also down-wasted by 15–20 m leading to the inferred transition of the glaciers from polythermal to cold-based thermal regimes (Carrivick et al., 2012).

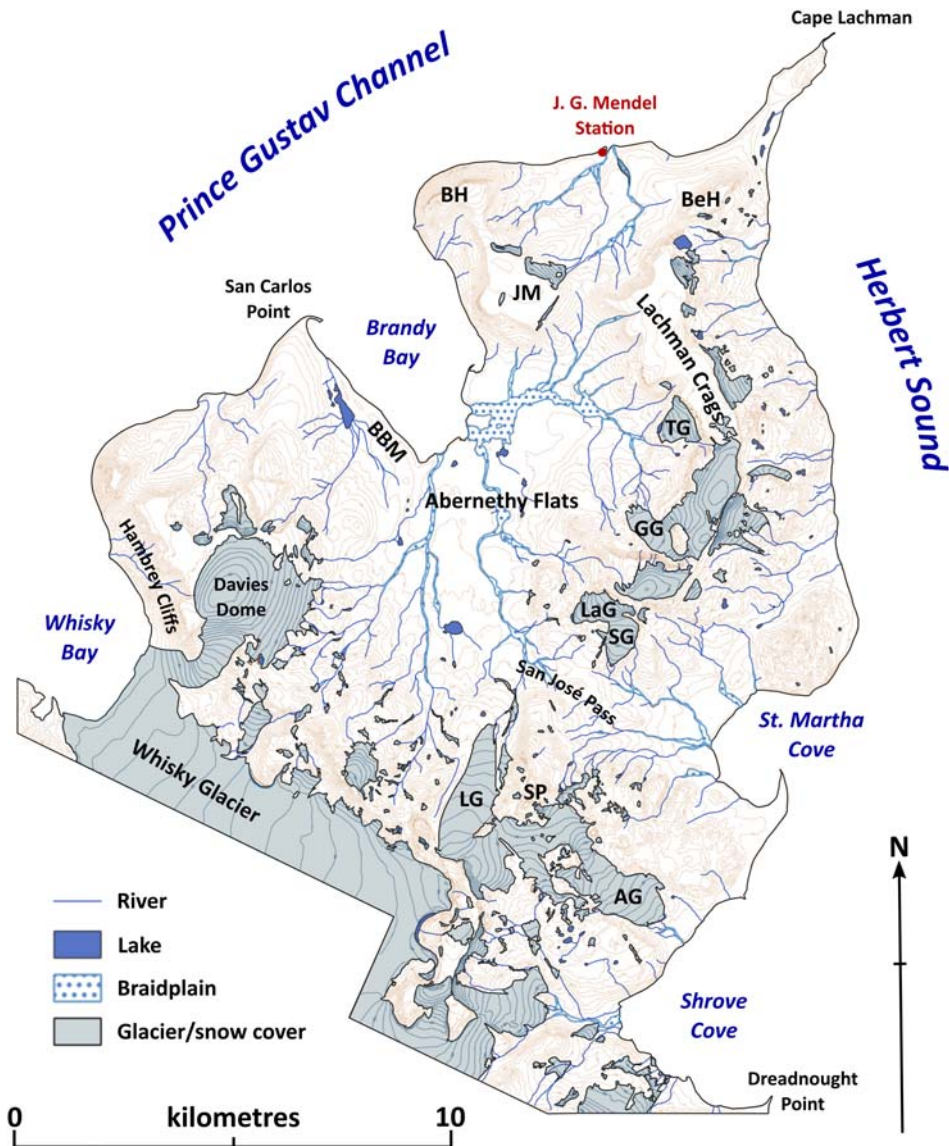


Figure 2. Topographic map of the northern sector of Ulu Peninsula illustrating the naming convention of key locations and localities mentioned in the text. BH: Bibby Hill; BeH: Berry Hill; JM: Johnson Mesa; TG: Triangular Glacier; GG: Glasser Glacier; BBM: Brandy Bay Moraine; LaG: Lachman Glacier; SG: San José Glacier; SP: Smellie Peak; LG: Lookalike Glacier; AG: Alpha Glacier.

The whole of the Ulu Peninsula is underlain by continuous permafrost (Bockheim et al., 2013; Obu et al., 2020), with an estimated thickness in coastal areas of c. 6–67 m (Borzotta & Trombotto, 2004). Active-layer thicknesses are strongly dependent on lithological properties but are usually in the range from 0.5 to 1.2 m. The near-surface ground thermal regime has a high occurrence of freeze–thaw cycles (Hrbáček et al., 2017), with the number of freeze–thaw cycles rapidly decreasing with depth, and typically no freeze–thaw activity being detected below depths of c. 20 cm (Hrbáček et al., 2017; Křážková et al., 2020). Unlike the relatively moist environment of the western Antarctic Peninsula, the land surface of the Ulu Peninsula can range from very dry to fully saturated, depending on the amount of snowpack meltwater available. This irregular surface wetting leads to the development of both aeolian features, such as desert pavements and surface cracks, as well

as periglacial landforms, such as sorted stripes and polygons (Davies et al., 2013).

3. Methods

Detailed geomorphological mapping was undertaken on-screen using a combination of ESRI ArcMap 10.6 and QGIS 3.2.3-Bonn Geographical Information System software, utilising British Antarctic Survey and Royal Navy aerial imagery, as well as the Reference Elevation Model of Antarctica (REMA) (Howat et al., 2019) (Figure 3). The aerial imagery of the central sector of the Ulu Peninsula was acquired by the British Antarctic Survey during 2006 using a Leica RC30 camera (Imagery A), with the northern sector imagery being acquired by the British Antarctic Survey during January 1979 using a Vinten 70 camera (Imagery B). This imagery was supplemented in the eastern Ulu Peninsula by imagery acquired by the Royal Navy in January 1989

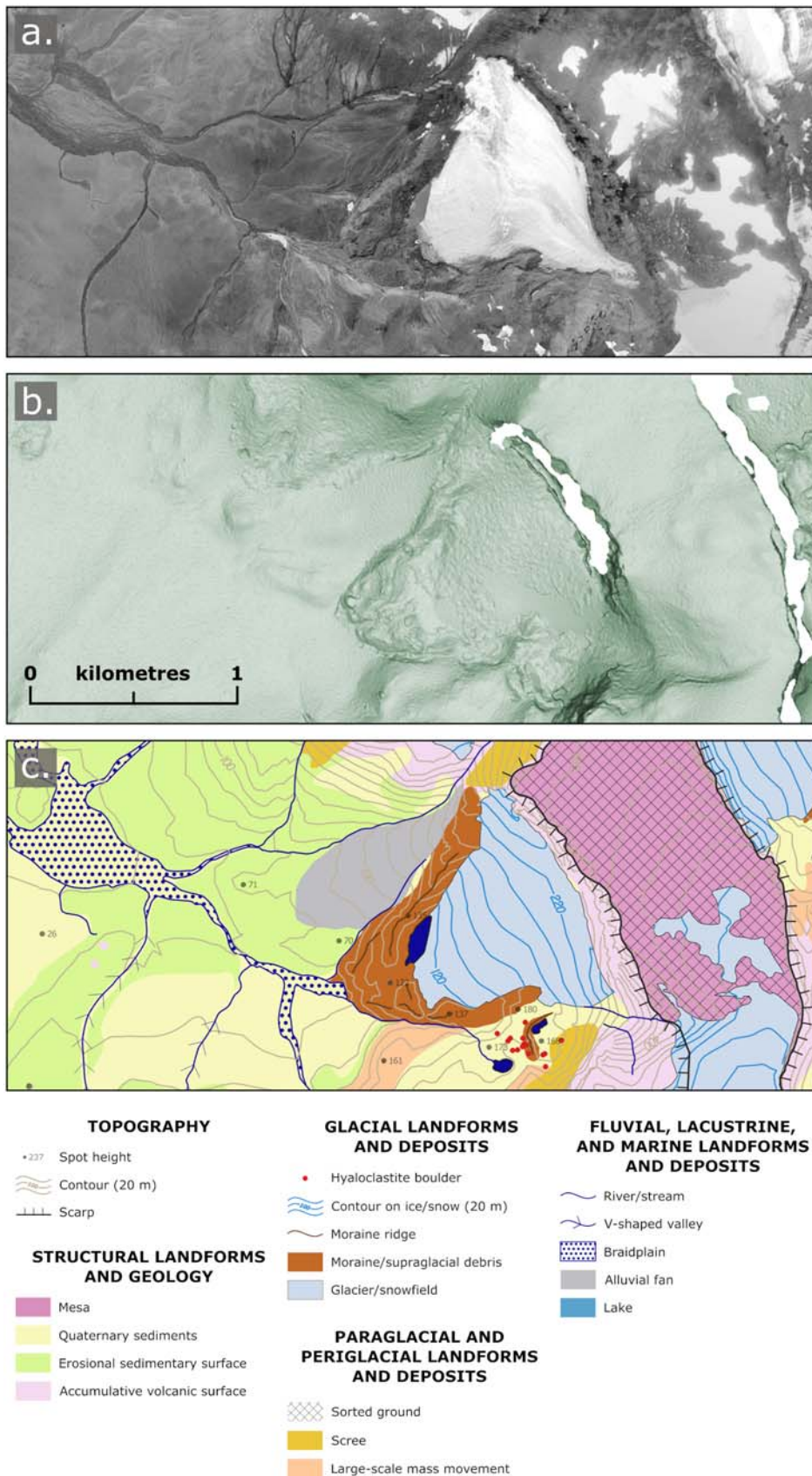


Figure 3. Comparison of the mapped geomorphological features with aerial imagery and the Reference Elevation Model of Antarctica (REMA) for Triangular Glacier and its proglacial area: (a) aerial imagery collected by the British Antarctic Survey during 2006 using a Leica RC30 camera; (b) slope map with 2 m resolution created from the Reference Elevation Model of Antarctica (REMA), note the blank areas are locations with no data (Howat et al., 2019); (c) geomorphological map with associated key below.

using a Zeiss RMK A camera (Imagery C). The scanned aerial imagery was processed using digital photogrammetric methods, with the planimetry and digital terrain model stereoplotted by GEODIS BRNO. The exterior orientations of the aerial imagery were calculated by aerotriangulation, and c. 80 ground control points situated at morphologically distinct locations were measured by dual frequency GPS, enabling orthorectification of the imagery. The resulting root mean square errors (RMSE) for each set of imagery were as follows: Imagery A – RMSE 0.70 m in plane, and 0.80 in height; Imagery B – RMSE 2.0 m in plane, and 2.0 m in height; Imagery C – RMSE 0.70 m in plane, 2.2 m in height (Czech Geological Survey, 2009).

Surface-feature and geomorphological mapping included the onscreen digitising of the coastline of Ulu Peninsula, the location of rivers and lakes, glacier extents and snow cover, geological components such as mesas, as well as a variety of relict and active geomorphological features and landforms. These features were verified by field observations in the austral summers of 2004 through to 2020. The identification of geomorphological (e.g. Davies et al., 2013; Yildirim, 2020) and glacially related landforms (e.g. Newall et al., 2020) in Antarctica from remotely-sensed imagery has already been well established, with Chandler et al. (2018) providing a comprehensive analysis of prevailing approaches and best practices. The geomorphological mapping of the northern Ulu Peninsula undertaken in this study combines new higher-resolution mapping at an unparalleled scale for the Antarctic Peninsula region. The characteristics of the main features mapped are described in the following sections.

Place names mentioned in this study follow the established naming convention after the SCAR Composite Gazetteer of Antarctica (2014).

4. Description of geomorphological features

Davies et al. 2013 has provided a detailed assessment of the geomorphological landforms present on the Ulu Peninsula, whereas a variety of other studies have investigated specific landforms (e.g. Ingólfsson et al., 1992; Hjort et al., 1997; Kavan et al., 2017; Křažková et al., 2020, 2021; Nedbalová et al., 2013; Strelin & Malagnino, 1992). Geomorphological features, geological components with morphological expressions, glaciological bodies, and glacial landforms have been mapped in this study. A brief overview of the main features mapped is included below to supplement the associated geomorphological map.

4.1. Basic map components

4.1.1. Coastline

The coastline of northern Ulu Peninsula is primarily bordered by beaches composed of sand or

cobbles/boulders (Figure 4(a)). Previously deposited glacial and fluvial sediments are reworked by long-shore currents, with, in places, a large number of boulders, which is typical of paraglacial environments (Ballantyne, 2002; Davies et al., 2013). Most of the boulders are erratic in origin, with further debris input derived from deposited glaciogenic materials that form steep slopes behind the beaches, which are subjected to erosion and solifluction (Davies et al., 2013). A notable area of coastline that is not fringed by beaches is located in Whisky Bay, where the terminal cliff of Whisky Glacier, a northwest-flowing tidewater glacier, calves into the ocean (Figure 2).

4.1.2. Glacier ice and snow

The ice masses on the northern sector of Ulu Peninsula are characterised by small cirque and valley glaciers that have become detached from source ice domes located on flat-topped volcanic mesas (Figure 4(c)) (Rabassa et al., 1982). These ice masses are dominated by continuous layering, interpreted as primary stratification (cf. Hambrey & Lawson, 2000), with a lack of major crevassing. This is typical of glaciers with a polythermal or cold-based regime and low throughputs, with only slow ice velocities. Supraglacial debris is commonly derived from precipitous side- and headwalls that deliver rockfall debris to the surface of the glaciers. Prominent ice-cored moraines are located in the proglacial zone, indicating the extent of the most recent glacial advance (Carrivick et al., 2012). These bear evidence of thrusts, suggesting that they were formed by polythermal glaciers.

Perennial snow banks are commonly formed in the lee of slopes where strong prevailing winds deposit aeolian transported snow. Melt from these snow banks often feed ephemeral streams and ephemeral to perennial lakes or ponds (Davies et al., 2013; Kavan et al., 2017, 2020).

4.1.3. Rivers, braidplains, and lakes

Ephemeral incised rivers and streams fed by perennial snowfields and glaciers are common on Ulu Peninsula (e.g. Kavan et al., 2017). These rivers are usually characterised by braidplains with multiple channels separated by small islands and bars (Figure 4(b)). Discharge is highly variable at diurnal, weekly, and seasonal timescales, with high discharge on positive degree-days able to rework glacial sediments and incise the Cretaceous strata (Davies et al., 2013; Kavan et al., 2017).

Numerous lakes, ponds, and seepages of different origins are scattered over the ice-free areas of the Ulu Peninsula (Lecomte et al., 2016; Nedbalová et al., 2013). They mostly form as a result of the

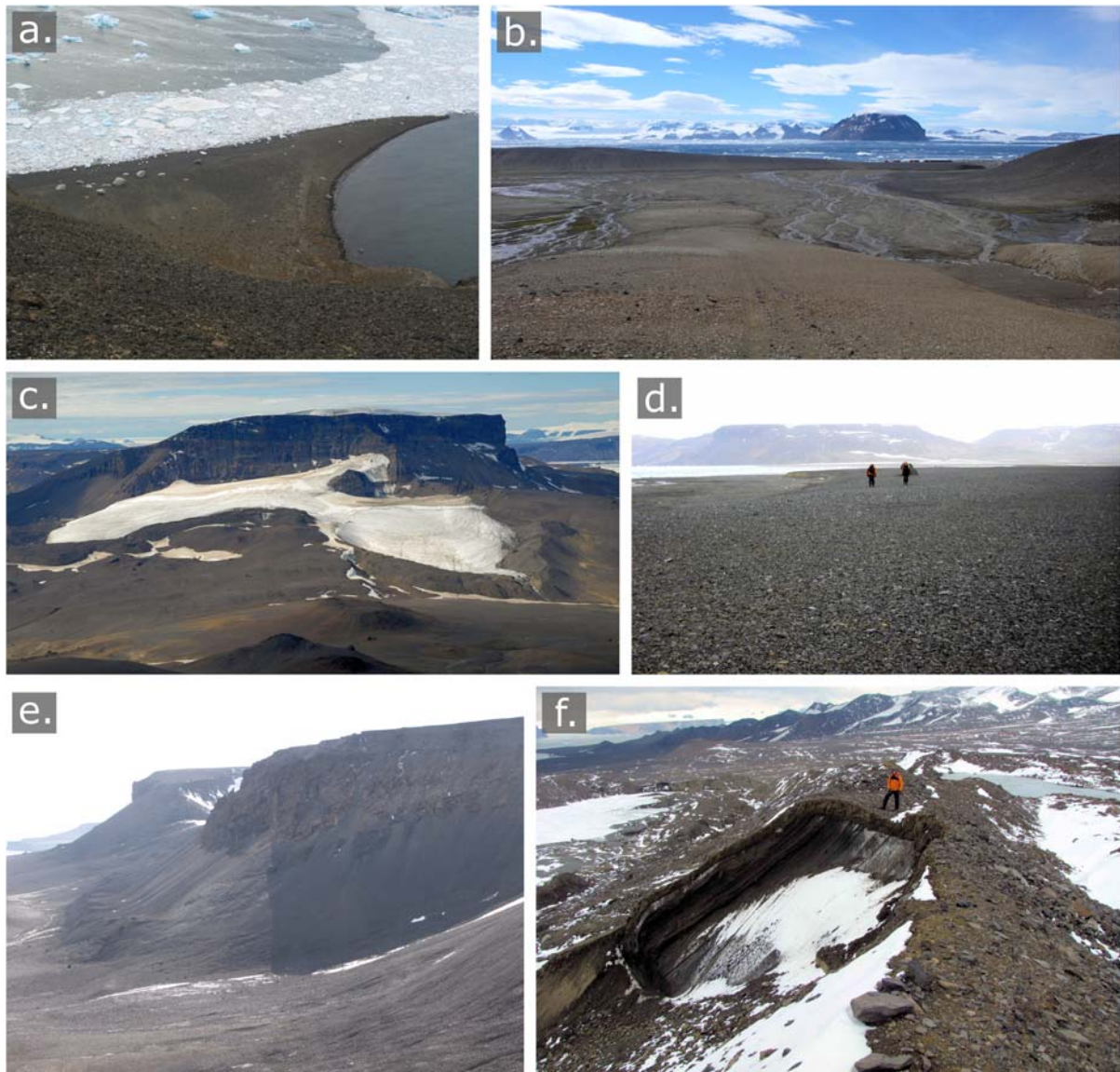


Figure 4. Key geomorphological features located on northern Ulu Peninsula including: (a) coastal spit located at Cape Lachman, composed of a sandy/cobble beach with granitic erratics originating from the Antarctic Peninsula; (b) ephemeral incised stream characterised by a braidplain, located to the south of J. G. Mendel station, photograph taken c. 1 km away from the station looking north; (c) two small valley glaciers, Lachman Glacier (left) and San José Glacier (right), located at the southern termination of the Lachman Crags, note the prominent flat-topped volcanic mesa behind the glaciers, and the steep ice-cored moraines in the proglacial zone, photograph taken from Smellie Peak facing towards the north; (d) marine terrace composed of rounded pebbles and a smooth flat surface, located near to the eastern shore of Brandy Bay, photograph taken facing towards the north with people for scale and Johnson Mesa in the background; (e) protalus ramparts situated beneath precipitous volcanic cliffs at the northern end of the Lachman Crags, note their curved profile with steep frontal slopes, photograph taken from Johnson Mesa looking north-east towards Berry Hill; (f) ice-cored moraine with an exposed ice section in the proglacial zone of San José Glacier, note the foliated ice and thin veneer of debris cover, photograph taken looking south-east towards Shrove Cove, person for scale. Photograph credits: images (a–c) – D. Nýlvt; images (d, e, and f) – B. Davies.

ablation of glacier ice, the melt of the snowpack, or because of isostatic uplift (Čejka et al., 2020; Lecomte et al., 2016; Nedbalová et al., 2013; Roman et al., 2019). Almost all precipitation falls as snow, which accumulates as large snowbanks during winter, and subsequently melts to form ephemeral seepages and large boggy areas of saturated ground in the summer months. Larger ponds and lakes also commonly have water sourced from ablating snowpack or glacier ice (Roman et al., 2019), and are usually perennial features

that freeze over during the winter, but become ice-free for at least part of the summer season.

4.2. Geological map components

4.2.1. Cretaceous to Neogene strata (erosional sedimentary surfaces)

James Ross Island mainly comprises Late Cretaceous poorly consolidated strata, composed of beds of mudstone (or mud) and sandstone (or sand) with spatially limited outcrops of fossiliferous marine sandstone,

shale, and conglomerate (Crame et al., 1991; Francis et al., 2006; Ineson et al., 1986). Similarly, poorly consolidated Late Miocene glaciogenic and glaciomarine diamictite and marine sandstone beds of Mendel Formation (Nývlt et al., 2011) crop out in the northernmost part of Ulu Peninsula. Previously mapped geological structures (Mlčoch et al., 2020) were used to determine the limits of the present erosional surfaces of the Cretaceous to Neogene basement rocks. The poorly consolidated Cretaceous strata are easily weathered and reworked by ice masses on Ulu Peninsula, as well as by ephemeral streams or wind activity (Carrivick et al., 2012; Kavan et al., 2017, 2020).

4.2.2. Volcanic landforms (accumulative volcanic surfaces)

Morphologically prominent volcanic mesas (flat-topped hills), such as the Lachman Crags and Johnson Mesa (see Figure 2 for locations), originated as a result of subglacial and subaqueous volcanic activity (Smellie et al., 2008, 2013). They are composed of steeply dipping foresets of hyaloclastite breccia covered by subaerial basalt topsets (Smellie, 2006), and in places, bottomset glaciogenic strata (Hambrey et al., 2008; Nehyba & Nývlt, 2015). Weathered basalt cover produces large blockfields with metre-scale basalt boulders on the surface of the mesas (2013). Minor tuff and cinder cones are also present (e.g. Bibby Hill), and represent volcanic activity in non-glacial marine conditions (Nehyba & Nývlt, 2014).

4.3. Geomorphological map components

4.3.1. Palaeoshorelines and marine limit

A series of palaeoshorelines and marine terraces are evident on James Ross Island. Marine terraces comprise smooth flat slopes, composed of rounded pebbles with a distinct lack of large boulders (Figure 4 (d)) (Davies et al., 2013). Marine terraces formed during and after deglaciation, reach a height of 90 m a.s.l., dating from the Pliocene through to the Holocene (Rabassa, 1983; Roberts et al., 2011). A marine limit of 30 m a.s.l. that is primarily observed in the Abernethy Flats (see Figure 2 for locations) has been suggested to be related to the deglaciation of the Prince Gustav Channel during the Pleistocene-Holocene transition (Hjort et al., 1997). However, some authors suggest that the 30 m terrace likely represents an earlier Quaternary marine limit, with a lower marine terrace of c. 16 m located in Brandy Bay correlating with the early-Holocene maximum, or ‘high stand’, of c. 15 m above present observed on Beak Island (cf. Roberts et al., 2011).

4.3.2. Scree and protalus ramparts

Scree slopes are common features located below steep Neogene basalt and hyaloclastite cliffs of volcanic mesas (Davies et al., 2013). Following recession after the Last Glacial Maximum, removal of the buttressing effect of the ice combined with the subaerial exposure of the cliffs left the rock strata susceptible to freeze-thaw action (Harris, 2007). The result was the formation of active scree slopes that provided an important debris source for rock glaciers, moraines, and protalus ramparts.

Protalus ramparts are features that form by the rolling of clasts down perennial snow banks, which are associated with scree. They form curved, flat landforms, with steep frontal slopes (Figure 4(e)).

4.3.3. Moraines

A range of different moraines with varying ages are present on Ulu Peninsula. The youngest of these moraines occur in the proglacial zone of small cirque and valley glaciers, indicating the maximum extent of their most recent advance (Carrivick et al., 2012). These moraines are ice-cored (Engel et al., 2012), with steep slopes and multiple sharp crests (Figure 4(f)). The debris composition varies; however, clasts range from subangular to subrounded, with the sediments ranging from sandy boulder gravel through to diamicton, according to the classification of Glasser (2011). Ice exposures in these moraines reveal foliated glacier ice that has been abandoned by the receding glaciers (Davies et al., 2013).

Older moraines are also evident on Ulu Peninsula, as can be seen on the south-western coastline of Brandy Bay. This ‘Brandy Bay Moraine’ is characterised by a c. 30 m high rounded ridgeline that runs for 3.5 km, with more rounded clasts than those found in ice-cored moraines (Davies et al., 2013, 2014; Hjort et al., 1997).

4.3.4. Rock glaciers

Rock glaciers often form below steep slopes or precipitous cliffs that act as a debris source (Figure 5(a)), and are composed of a mixture of debris and ice, that form lobate landforms with steep lateral and terminal margins (Humlum, 2000). Numerous glacier-derived rock glaciers are located on the eastern slopes of the Lachman Crags, facing towards Herbert Sound (Fukui et al., 2007, 2008).

4.3.5. Large-scale mass movements

Large-scale mass movements are present on Ulu Peninsula as a result of James Ross Volcanic Group rocks overlying gently inclined and poorly consolidated Cretaceous strata. The removal of the buttressing effect provided either by glacier ice or marine hydraulic pressure subsequent to deglaciation or isostatic uplift respectively, resulted in the destabilisation



Figure 5. Key geomorphological features located on northern Ulu Peninsula including: (a) rock glacier situated below the south-eastern flank of Berry Hill, flowing towards Herbert Sound, photographed from Vega Island looking west; (b) large-scale mass movement that became separated from the eastern side of the Lachman Crag, photograph taken towards the south-east with Herbert Sound in the background; (c) crystalline erratic boulders (up to several metres in diameter) located on the coastal spit at Cape Lachman that have been glacially transported from the Antarctic Peninsula, photograph taken from the end of the spit looking south-west towards Ulu Peninsula; (d) detailed image of a hyaloclastite boulder in the boulder train that runs from the western side of Lookalike Glacier to the western side of Brandy Bay, note the compass-clinometer for scale; (e) well developed polygons with boundaries further highlighted by lichens (black) on top of Johnson Mesa, geological hammer for scale; (f) stone stripes that develop on slopes as a result of freeze-thaw activity, located on the northern slopes of Berry Hill, stripes in the photograph range from several tens of centimetres through to c. 1 m in width. Photograph credits: images (a, b, e, and f) – D. Nývlt; image (c) – B. Mlčoch; image (d) – M. Hambrey.

of steep delta fronts and ensuing downslope mass movement of large basalt blocks (Davies et al., 2013). Detached volcanic blocks with dimensions ranging from tens to hundreds of metres (Figure 5(b)) form chaotic terrain, often with rotated geological horizons (e.g. Calabozo et al., 2015).

4.3.6. Crystalline and hyaloclastite boulders

Crystalline erratics (Figure 5(c)) are present all over the Ulu Peninsula, deposited during the Neogene and Quaternary glaciations that inundated James Ross Island (Davies et al., 2013; Nývlt et al., 2011; 2014). The lithological differences between James Ross Island and the mainland Antarctic Peninsula illustrate that these granitic and phyllite clasts must have been derived from the Antarctic Peninsula, as these lithologies are absent as bedrock on Ulu Peninsula. The presence of erratics on the top of mesas suggests that they were once overridden by glacier ice derived from the Antarctic Peninsula (Glasser et al., 2014). Alternatively, the erratics may be derived from ice-rafted debris that was subaqueously deposited during the Neogene (Smellie et al., 2008).

In contrast to the crystalline erratics, hyaloclastite boulders (Figure 5(d)) are locally derived from the Ulu Peninsula. The most striking example of hyaloclastite boulders is a train of large boulders running from the western side of Lookalike Glacier to the western side of Brandy Bay (Björck et al., 1996; Davies et al., 2013; Hjort et al., 1997; Kňázková et al., 2020).

4.3.7. Solifluction lobes

Solifluction lobes occur on many moderate to low-angled slopes and are also active in the modification of ice-cored moraines. Freeze–thaw activity results in the downslope gravitational deformation of material by frost creep (Harris, 2007). As a result, solifluction, along with other slope processes, reduce slope gradients (Davies et al., 2013).

4.3.8. Sorted ground

Modification of surfaces by freeze–thaw activity results in the development of features such as polygons, stone stripes, and thermal contraction cracks (Figure 5(e,f)). Polygons have diameters that range from 0.5 to 4.0 m, and are especially evident in areas of higher water content, but also develop on the top of mesas. Polygons and stone stripes develop in response to diurnal freezing and thawing on flat and inclined surfaces respectively (Ballantyne, 2007). Thermal contraction cracks develop as a result of seasonal temperature changes where frozen ground experiences thermal tension and fissuring (Ballantyne, 2002; Levy et al., 2008).

5. Discussion and conclusions

This study documents the geomorphology of a deglaciated area of the Antarctic Peninsula integrating geology, glaciology, and Earth-surface processes.

The variety of geomorphology on the Ulu Peninsula reflects the geological characteristics of the area, but it also highlights a wide array of Earth-surface processes. The broad landscape characteristics are in part, determined by the underlying geology, which has been sculpted by overlying ice masses during numerous glacial periods (Bentley & Anderson 1998; Camerlenghi et al., 2001; Davies et al., 2012b; Evans et al., 2005; Glasser et al., 2014; Heroy & Anderson, 2007; Johnson et al., 2011; Kaplan et al., 2020; Mulvaney et al., 2012). Both paraglacial and periglacial features are superimposed upon the glacially-moulded landscape, reflecting the landscape evolution following deglaciation (Davies et al., 2013; Ruiz-Fernández et al., 2019).

At present, the study area can be broadly separated into three zones defined by the dominant geomorphological processes, comprising a southern glacierised sector, a paraglacial eastern sector (to the east of the Lachman Crags), with a periglacially dominated central and northern sectors (Abernethy Flats area, and the area surrounding J. G. Mendel Station). The glacial sector encompasses the largest ice masses on northern Ulu Peninsula, including Whisky Glacier, Davies Dome, and the valley glaciers Lookalike Glacier and Alpha Glacier (see Figure 2 for locations).

The paraglacial sector comprises a number of large-scale mass movements. These mass movements have a geological control, with the instability most likely being derived from deglaciation or isostatic uplift. Despite the period of time that has passed since deglaciation, this process is still active, as evidenced by the subsidence of a large volcanic slab by several tens of metres on the eastern side of the Lachman Crags (Davies et al., 2013).

The central and northern sectors of the study area are dominated by periglacial processes, with freeze–thaw cycles in the active layer leading to the development of polygons, stone stripes, and thermal contraction cracks (Ballantyne, 2007; Kňázková et al., 2020; Levy et al., 2008).

The geomorphological map presented in this study covers an area more than one order of magnitude larger than other previously published maps from other Antarctic Peninsula and South Shetland Island areas (e.g. López-Martínez et al., 1996, 2012; Martín-Serrano et al., 2005; Yildirim, 2020). The unique opportunity to study Antarctic geomorphological processes on such a large scale facilitates a broader understanding of the evolution and interactions between palaeoglaciological, paraglacial, and periglacial features. This study records the complex and dynamic history of the Ulu Peninsula area following

deglaciation, and it is anticipated that it will provide a foundation for future multidisciplinary studies. Furthermore, as the Antarctic Peninsula deglaciates, landscapes similar to the Ulu Peninsula will become increasingly common, therefore, understanding the current evolution of the Ulu Peninsula may provide clues for predicting potential future changes for other areas in the Antarctic Peninsula region.

Software

Initial map production was undertaken using ESRI ArcMap 10.6 and QGIS 3.2.3-Bonn Geographical Information System software, with further map/figure manipulation conducted in Inkscape version 0.92.3.

Acknowledgements

The authors thank Dominic A. Hodgson, Kelly Hogan, and Chris Orton for their helpful comments on the manuscript and accompanying map, and Paul Dunlop for editing.

Data availability statement

The authors confirm that the data supporting the findings of this study are available within the article and its supplementary materials.

Disclosure statement

No potential conflict of interest was reported by the author(s).

Funding

This work was supported from Operational Programme Research, Development, and Education - Project Postdoc@MUNI (No. CZ.02.2.69/0.0/0.0/16_027/0008360), by infrastructural projects supporting the operation of the J. G. Mendel Station (LM2015078 and VAN2020/1), and was partly supported by the project NUNANTAR (02/SAICT/2017–32002; Fundação para a Ciência e a Tecnologia, Portugal). Fieldwork was also funded by the UK Natural Environment Research Council (NERC) under the Antarctic Funding Initiative (NE/F012942/1). Transport, logistics, and fieldwork on James Ross Island for BJD, NFG, JLC, and MJH were supported by the British Antarctic Survey and the Royal Navy, and we thank the captain and crew of the RRS *Ernest Shackleton*, the RRS *James Clark Ross*, and HMS *Protector* for their support.

ORCID

Stephen J. A. Jennings  <http://orcid.org/0000-0003-4255-4522>

Bethan J. Davies  <http://orcid.org/0000-0002-8636-1813>

Daniel Nývlt  <http://orcid.org/0000-0002-6876-490X>

Neil F. Glasser  <http://orcid.org/0000-0002-8245-2670>

Zbyněk Engel  <http://orcid.org/0000-0002-5209-7823>

Filip Hrbáček  <http://orcid.org/0000-0001-5032-9216>

Jonathan L. Carrivick  <http://orcid.org/0000-0002-9286-5348>

Michael J. Hambrey  <http://orcid.org/0000-0003-0662-1783>

References

- Ambrozova, K., Láska, K., Hrbáček, F., Kavan, J., & Ondruch, J. (2019). Air temperature and lapse rate variation in the ice-free and glaciated areas of northern James Ross Island, Antarctic Peninsula, during 2013–2016. *International Journal of Climatology*, 39(2), 643–657. <https://doi.org/10.1002/joc.5832>
- Balco, G., Schaefer, J. M., & LARISSA Group. (2013). Exposure-age record of Holocene ice sheet and ice shelf change in the northeast Antarctic Peninsula. *Quaternary Science Reviews*, 59, 101–111. <https://doi.org/10.1016/j.quascirev.2012.10.022>
- Ballantyne, C. K. (2002). Paraglacial geomorphology. *Quaternary Science Reviews*, 21(18–19), 1935–2017. [https://doi.org/10.1016/S0277-3791\(02\)00005-7](https://doi.org/10.1016/S0277-3791(02)00005-7)
- Ballantyne, C. K. (2007). Periglacial landforms: Patterned ground. In S. A. Elias (Ed.), *Encyclopedia of Quaternary Science* (pp. 2182–2191). Elsevier.
- Barrand, N. E., Vaughan, D. G., Steiner, N., Tedesco, M., Kuipers Munneke, P., van den Broeke, M. R., & Hosking, J. S. (2013). Trends in Antarctic Peninsula surface melting conditions from observations and regional climate modelling. *Journal of Geophysical Research: Earth Surface*, 118(1), 315–330. <https://doi.org/10.1029/2012JF002559>
- Bentley, M. J., & Anderson, J. B. (1998). Glacial and marine geological evidence for the ice sheet configuration in the Weddell Sea-Antarctic Peninsula region during the Last Glacial Maximum. *Antarctic Science*, 10(3), 309–325. <https://doi.org/10.1017/S0954102098000388>
- Bentley, M. J., Fogwill, C. J., Kubik, P. W., & Sugden, D. E. (2006). Geomorphological evidence and cosmogenic ¹⁰Be/²⁶Al exposure ages for the Last Glacial Maximum and deglaciation of the Antarctic Peninsula Ice Sheet. *Geological Society of America Bulletin*, 118(9–10), 1149–1159. <https://doi.org/10.1130/B25735.1>
- Björck, S., Olsson, S., Ellis-Evans, C., Håkansson, H., Humlum, O., & De Lirio, J. M. (1996). Late Holocene palaeoclimatic records from lake sediments on James Ross Island, Antarctica. *Palaeogeography, Palaeoclimatology, Palaeoecology*, 121(3–4), 195–220. [https://doi.org/10.1016/0031-0182\(95\)00086-0](https://doi.org/10.1016/0031-0182(95)00086-0)
- Bockheim, J., Vieira, G., Ramos, M., López-Martínez, J., Serrano, E., Guglielmin, M., Wilhelm, K., & Nieuwendam, A. (2013). Climate warming and permafrost dynamics in the Antarctic Peninsula region. *Global and Planetary Change*, 100, 215–223. <https://doi.org/10.1016/j.globplacha.2012.10.018>
- Borzotta, E., & Trombotto, D. (2004). Correlation between frozen ground thickness measured in Antarctica and permafrost thickness estimated on the basis of the heat flow obtained from magnetotelluric soundings. *Cold Regions Science and Technology*, 40(1–2), 81–96. <https://doi.org/10.1016/j.coldregions.2004.06.002>
- British Antarctic Survey. (2017). Northern Antarctic Peninsula. *Series BAS (UKAHT) Sheets 3A and 3B, 1:250 000*, Cambridge.
- Calabozo, F. M., Strelin, J. A., Orihashi, Y., Sumino, H., & Keller, R. A. (2015). Volcano-ice-sea interaction in the Cerro Santa Marta area, northwest James Ross Island,

- Antarctic Peninsula. *Journal of Volcanology and Geothermal Research*, 297, 89–108. <https://doi.org/10.1016/j.jvolgeores.2015.03.011>
- Camerlenghi, A., Domack, E., Rebesco, M., Gilbert, R., Ishman, S., Leventer, A., Brachfeld, S., & Drake, A. (2001). Glacial morphology and post-glacial contourites in northern Prince Gustav Channel (NW Weddell Sea. *Marine Geophysical Researches*, 22(5/6), 417–443. <https://doi.org/10.1023/A:1016399616365>
- Carrivick, J. L., Davies, B. J., Glasser, N. F., Nývlt, D., & Hambrey, M. J. (2012). Late-Holocene changes in character and behaviour of land-terminating glaciers on James Ross Island, Antarctica. *Journal of Glaciology*, 58(212), 1176–1190. <https://doi.org/10.3189/2012JoG11J148>
- Čejka, T., Nývlt, D., Kopalová, K., Bulínová, M., Kavan, J., Lirio, J. M., Coria, S. H., & van de Vijver, B. (2020). Timing of the neoglaciation onset of the north-eastern Antarctic Peninsula based on lacustrine archives from Lake Anónima, Vega Island. *Global and Planetary Change*, 184, 103050. <https://doi.org/10.1016/j.gloplacha.2019.103050>
- Chandler, B. M. P., Lovell, H., Boston, C. M., Lukas, S., Barr, I. D., Benediktsson, Í. Ó., Benn, D. I., Clark, C. D., Darvill, C. M., Evans, D. J. A., Ewertowski, M. W., Loibl, D., Margold, M., Otto, J.-C., Roberts, D. H., Stokes, C. R., Storrar, R. D., & Stroeven, A. P. (2018). Glacial geomorphological mapping: A review of approaches and frameworks for best practice. *Earth-Science Reviews*, 185, 806–846. <https://doi.org/10.1016/j.earscirev.2018.07.015>
- Charman, D. J., Amesbury, M. J., Roland, T. P., Royles, J., Hodgson, D. A., Convey, P., & Griffiths, H. (2018). Spatially coherent late Holocene Antarctic Peninsula surface air temperature variability. *Geology*, 46(12), 1071–1074. <https://doi.org/10.1130/G45347.1>
- Cofaigh C. Ó., Davies, B. J., Livingstone, S. J., Smith, J. A., Johnson, J. S., Hocking, E. P., Hodgson, D. A., Anderson, J. B., Bentley, M. J., Canals, M., Domack, E., Dowdeswell, J. A., Evans, J., Glasser, N. F., Hillenbrand, C.-D., Larter, R. D., Roberts, S. J., & Simms, A. R. (2014). Reconstruction of ice-sheet changes in the Antarctic Peninsula since the Last Glacial Maximum. *Quaternary Science Reviews*, 100, 87–110. <https://doi.org/10.1016/j.quascirev.2014.06.023>
- Cook, A. J., Fox, A. J., Vaughan, D. G., & Ferrigno, J. G. (2005). Retreating glacier fronts on the Antarctic Peninsula over the past half-century. *Science*, 308(5721), 541–544. <https://doi.org/10.1126/science.1104235>
- Cook, A. J., & Vaughan, D. G. (2010). Overview of areal changes of the ice shelves on the Antarctic Peninsula over the past 50 years. *The Cryosphere*, 4(1), 77–98. <https://doi.org/10.5194/tc-4-77-2010>
- Crame, J. A., Pirrie, D., Riding, J. B., & Thomson, M. R. A. (1991). Campanian-Maastrichtian (Cretaceous) stratigraphy of the James Ross Island area, Antarctica. *Journal of the Geological Society*, 148(6), 1125–1140. <https://doi.org/10.1144/gsjgs.148.6.1125>
- Czech Geological Survey. (2009). *James Ross Island – Northern Part. Topographic Map 1:25 000*.
- Davies, B. J., Carrivick, J. L., Glasser, N. F., Hambrey, M. J., & Smellie, J. L. (2012a). Variable glacier response to atmospheric warming, northern Antarctic Peninsula, 1988–2009. *The Cryosphere*, 6(5), 1031–1048. <https://doi.org/10.5194/tc-6-1031-2012>
- Davies, B. J., Glasser, N. F., Carrivick, J. L., Hambrey, M. J., Smellie, J. L., & Nývlt, D. (2013). Landscape evolution and ice-sheet behaviour in a semi-arid polar environment: James Ross Island, NE Antarctic Peninsula. In M. J. Hambrey, P. F. Barker, P. J. Barrett, V. C. Bowman, B. J. Davies, J. L. Smellie, & M. Tranter (Eds.), *Antarctic palaeoenvironments and Earth surface processes* (vol., 381, pp. 353–395). Geological Society of London, Special Publication.
- Davies, B. J., Gollidge, N. R., Glasser, N. F., Carrivick, J. L., Ligtenberg, S. R. M., Barrand, N. E., van den Broeke, M. R., Hambrey, M. J., & Smellie, J. L. (2014). Modelled glacier response to centennial temperature and precipitation trends on the Antarctic Peninsula. *Nature Climate Change*, 4(11), 993–998. <https://doi.org/10.1038/nclimate2369>
- Davies, B. J., Hambrey, M. J., Smellie, J. L., Carrivick, J. L., & Glasser, N. F. (2012b). Antarctic Peninsula ice sheet evolution during the Cenozoic Era. *Quaternary Science Reviews*, 31, 30–66. <https://doi.org/10.1016/j.quascirev.2011.10.012>
- Dickens, W. A., Kuhn, G., Leng, M. J., Graham, A. G. C., Dowdeswell, J. A., Meredith, M. P., Hillenbrand, C.-D., Hodgson, D. A., Roberts, S. J., Sloane, H., & Smith, J. A. (2019). Enhanced glacial discharge from the eastern Antarctic Peninsula since the 1700s associated with a positive Southern Annular Mode. *Scientific Reports*, 9(1), 14606. <https://doi.org/10.1038/s41598-019-50897-4>
- Engel, Z., Láska, K., Nývlt, D., & Stachoň, Z. (2018). Surface mass balance of small glaciers on James Ross Island, north-eastern Antarctic Peninsula, during 2009–2015. *Journal of Glaciology*, 64(245), 349–361. <https://doi.org/10.1017/jog.2018.17>
- Engel, Z., Nývlt, D., & Láska, K. (2012). Ice thickness, areal and volumetric changes of Davies Dome and Whisky Glacier (James Ross Island, Antarctic Peninsula) in 1979–2006. *Journal of Glaciology*, 58(211), 904–914. <https://doi.org/10.3189/2012JoG11J156>
- Evans, J., Pudsey, C. J., Cofaigh C. Ó., Morris, P., & Domack, E. (2005). Late Quaternary glacial history, flow dynamics and sedimentation along the eastern margin of the Antarctic Peninsula Ice Sheet. *Quaternary Science Reviews*, 24(5–6), 741–774. <https://doi.org/10.1016/j.quascirev.2004.10.007>
- Francis, J. E., Pirrie, D., & Crame, J. A. (2006). *Cretaceous-Tertiary high-latitude palaeoenvironments: James Ross basin, Antarctica*, (p. 258). Geological Society of London, Special Publication.
- Fukui, K., Sone, T., Strelin, J., Torielli, C., & Mori, J. (2007). Ground penetrating radar sounding on an active rock glacier on James Ross Island, Antarctic Peninsula region. *Polish Polar Research*, 28(1), 13–22.
- Fukui, K., Sone, T., Strelin, J. A., Torielli, C. A., Mori, J., & Fujii, Y. (2008). Dynamics and GPR stratigraphy of a polar rock glacier on James Ross Island, Antarctic Peninsula. *Journal of Glaciology*, 54(186), 445–451. <https://doi.org/10.3189/002214308785836940>
- Glasser, N. F., Davies, B. J., Carrivick, J. L., Rodés, A., Hambrey, M. J., Smellie, J. L., & Domack, E. (2014). Ice-stream initiation, duration and thinning on James Ross Island, northern Antarctic Peninsula. *Quaternary Science Reviews*, 86, 78–88. <https://doi.org/10.1016/j.quascirev.2013.11.012>
- Glasser, N. F., Kulesa, B., Luckman, A., Jansen, D., King, E. C., Sammonds, P. R., Scambos, T. A., & Jezek, K. C. (2009). Surface structure and stability of the Larsen C Ice Shelf, Antarctic Peninsula. *Journal of Glaciology*, 55(191), 400–410. <https://doi.org/10.3189/00221430978816597>
- Hambrey, M. J., & Glasser, N. F. (2011). Sediment entrainment, transfer and deposition. In V. P. Singh, P. Singh, &

- U. K. Haritashya (Eds.), *Encyclopedia of snow, ice and glaciers* (pp. 984–1003). Springer.
- Hambrey, M. J., & Lawson, W. J. (2000). Structural styles and deformation fields in glaciers: A review. In A. J. Maltman, B. Hubbard, & M. J. Hambrey (Eds.), *Deformation of glacial materials*, (p. 59–83) Geological Society of London, Special Publications, 176.
- Hambrey, M. J., & Smellie, J. L. (2006). Distribution, lithofacies and environmental context of Neogene glacial sequences on James Ross and Vega islands, Antarctic peninsula. *Geological Society, London, Special Publications*, 258(1), 187–200. <https://doi.org/10.1144/GSL.SP.2006.258.01.14>
- Hambrey, M. J., Smellie, J. L., Nelson, A. E., & Johnson, J. S. (2008). Late Cenozoic glacier-volcano interaction on James Ross Island and adjacent areas, Antarctic Peninsula region. *Geological Society of America Bulletin*, 120(5–6), 709–731. <https://doi.org/10.1130/B26242.1>
- Harris, C. (2007). Periglacial landforms: Slope deposits and forms. In A. E. Scott (Ed.), *Encyclopaedia of quaternary science* (pp. 2207–2217). Elsevier.
- Heroy, D. C., & Anderson, J. B. (2007). Radiocarbon constraints on Antarctic Peninsula ice sheet retreat following the last glacial maximum (LGM). *Quaternary Science Reviews*, 26(25–28), 3286–3297. <https://doi.org/10.1016/j.quascirev.2007.07.012>
- Hjort, C., Ingólfsson, Ó, Möller, P., & Lirio, J. M. (1997). Holocene glacial history and sea-level changes on James Ross Island. *Antarctic Peninsula. Journal of Quaternary Science*, 12(4), 259–273. [https://doi.org/10.1002/\(SICI\)1099-1417\(199707/08\)12:4<259::AID-JQS307>3.0.CO;2-6](https://doi.org/10.1002/(SICI)1099-1417(199707/08)12:4<259::AID-JQS307>3.0.CO;2-6)
- Hodgson, D. A. (2011). First synchronous retreat of ice shelves marks a new phase of polar deglaciation. *Proceedings of the National Academy of Sciences*, 108(47), 18859–18860. <https://doi.org/10.1073/pnas.1116515108>
- Howat, I. M., Porter, C., Smith, B. E., Noh, M.-J., & Morin, P. (2019). The reference elevation model of Antarctica. *The Cryosphere*, 13(2), 665–674. <https://doi.org/10.5194/tc-13-665-2019>
- Hrbáček, F., Nývlt, D., & Láška, K. (2017). Active layer thermal dynamics at two lithologically different sites on James Ross Island, eastern Antarctic Peninsula. *Catena*, 149(2), 592–602. <https://doi.org/10.1016/j.catena.2016.06.020>
- Humlum, O. (2000). The geomorphic significance of rock glaciers: Estimates of rock glacier debris volumes and headwall recession rates in west Greenland. *Geomorphology*, 35(1-2), 41–67. [https://doi.org/10.1016/S0169-555X\(00\)00022-2](https://doi.org/10.1016/S0169-555X(00)00022-2)
- Ineson, J. R., Crame, J. A., & Thomson, M. R. A. (1986). Lithostratigraphy of the cretaceous strata of west James Ross Island, Antarctica. *Cretaceous Research*, 7(2), 141–159. [https://doi.org/10.1016/0195-6671\(86\)90014-5](https://doi.org/10.1016/0195-6671(86)90014-5)
- Ingólfsson, Ó, Hjort, C., Björck, S., & Smith, L. (1992). Late Pleistocene and Holocene glacial history of James Ross Island. *Antarctic Peninsula. Boreas*, 21(3), 209–222. <https://doi.org/10.1111/j.1502-3885.1992.tb00029.x>
- Johnson, J. S., Bentley, M. J., Roberts, S. J., Binney, S. A., & Freeman, S. P. H. T. (2011). Holocene deglacial history of the north east Antarctic Peninsula – a review and new chronological constraints. *Quaternary Science Reviews*, 30(27-28), 3791–3802. <https://doi.org/10.1016/j.quascirev.2011.10.011>
- Kaplan, M. R., Strelin, J. A., Schaefer, J. M., Peltier, C., Martini, M. A., Flores, E., Winckler, G., & Schwartz, R. (2020). Holocene glacier behavior around the northern Antarctic Peninsula and possible causes. *Earth and Planetary Science Letters*, 534, 116077. <https://doi.org/10.1016/j.epsl.2020.116077>
- Kavan, J., Nývlt, D., Láška, K., Engel, Z., & Kňazková, M. (2020). High-latitude dust deposition in snow on the glaciers of James Ross Island, Antarctica. *Earth Surface Processes and Landforms*, 45(7), 1569–1578. <https://doi.org/10.1002/esp.4831>
- Kavan, J., Ondruch, J., Nývlt, D., Hrbáček, F., Carrivick, J. L., & Láška, K. (2017). Seasonal hydrological and suspended sediment transport dynamics in proglacial streams, James Ross Island, Antarctica. *Geografiska Annaler: Series A, Physical Geography*, 99(1), 38–55. <https://doi.org/10.1080/04353676.2016.1257914>
- Kňazková, M., Hrbáček, F., Kavan, J., & Nývlt, D. (2020). Effect of hyaloclastite breccia boulders on meso-scale periglacial-aeolian landsystem in semi-arid Antarctic environment, James Ross Island, Antarctic Peninsula. *Cuadernos de Investigación Geográfica*, 46(1), 7–31. <https://doi.org/10.18172/cig.3800>
- Kňazková, M., Nývlt, D., & Hrbáček, F. (2021). Slope processes connected with snow patches in semi-arid ice-free areas of James Ross Island, Antarctic Peninsula. *Geomorphology*, 373, 107479. <https://doi.org/10.1016/j.geomorph.2020.107479>
- Lecomte, K. L., Vignoni, P. A., Córdoba, F. E., Chaparro, M. A. E., Kopalová, K., Gargiulo, J. D., Lirio, J. M., Irurzun, M. A., & Böhnell, H. N. (2016). Hydrological systems from the Antarctic Peninsula under climate change: James Ross archipelago as study case. *Environmental Earth Sciences*, 75(7), 623. <https://doi.org/10.1007/s12665-016-5406-y>
- Lee, J. R., Raymond, B., Bracegirdle, T. J., Chadès, I., Fuller, R. A., Shaw, J. D., & Terauds, A. (2017). Climate change drives expansion of Antarctic ice-free habitat. *Nature*, 547(7661), 49–54. <https://doi.org/10.1038/nature22996>
- Levy, J. S., Head, J. W., & Marchant, D. R. (2008). The role of thermal contraction crack polygons in cold-desert fluvial systems. *Antarctic Science*, 20(6), 565–579. <https://doi.org/10.1071/S0954102008001375>
- López-Martínez, J., Serrano, E., Schmid, T., Mink, S., & Linés, C. (2012). Periglacial processes and landforms in the South Shetland Islands (northern Antarctic Peninsula region). *Geomorphology*, 155-156, 62–79. <https://doi.org/10.1016/j.geomorph.2011.12.018>
- López-Martínez J, Thomson MRA, Arche A, Björck S, Ellis-Evans JC, Hathway B, Hernández-Cifuentes F, Hjort C, Ingólfsson Ó, Ising J, Lomas S, Martínez de Pisón, Serrano E, Zale R and King S (1996) *Geomorphological map of Byers Peninsula, Livingston Island*. BAS GEOMAP Series, Sheet 5-A, 1:25 000 with supplementary text, Cambridge.
- Lundquist, J., Lilliesköld, M., & Ostmark, K. (1995). Glacial and periglacial deposits of the Tumbledown Cliffs area, James Ross Island, West Antarctica. *Geomorphology*, 11(3), 205–214. [https://doi.org/10.1016/0169-555X\(94\)00051-R](https://doi.org/10.1016/0169-555X(94)00051-R)
- Martín-Serrano, A., Montes, M., Nozal Martín, F., & del Valle, R. (2005). Geomorfología de la costa austral de bahía esperanza (Península Antártica). *Geogaceta*, 38, 95–98.
- Mlčoch, B., Nývlt, D., & Mixa, P. (2020). *Geological map of James Ross Island - northern part. 1:25 000, Czech Geological Survey*. Praha.
- Mulvaney, R., Abram, N. J., Hindmarsh, R. C. A., Arrowsmith, C., Fleet, L., Triest, J., Sime, L. C., Alemany, O., & Foord, S. (2012). Recent Antarctic

- Peninsula warming relative to Holocene climate and ice-shelf history. *Nature*, 489(7414), 141–144. <https://doi.org/10.1038/nature11391>
- Nedbalová, L., Nývlt, D., Kopáček, J., Šobr, M., & Elster, J. (2013). Freshwater lakes of Ulu Peninsula, James Ross Island, north-east Antarctic Peninsula: Origin, geomorphology and physical and chemical limnology. *Antarctic Science*, 25(3), 358–372. <https://doi.org/10.1017/S0954102012000934>
- Nehyba, S., & Nývlt, D. (2014). Deposits of pyroclastic mass flows at Bibby Hill (Pliocene, James Ross Island, Antarctica). *Czech Polar Reports*, 4(2), 103–122. <https://doi.org/10.5817/CPR2014-2-11>
- Nehyba, S., & Nývlt, D. (2015). ‘Bottomsets’ of the lava-fed delta of James Ross Island Volcanic Group, Ulu Peninsula, James Ross Island, Antarctica. *Polish Polar Research*, 36(1), 1–24. <https://doi.org/10.1515/popore-2015-0002>
- Nelson, A. E., Smellie, J. L., Hambrey, M. J., Williams, M., Vautravers, M., Salzmann, U., McArthur, J. M., & Regelous, M. (2009). Neogene glacial debris flows on James Ross Island, northern Antarctic Peninsula, and their implications for regional climate history. *Quaternary Science Reviews*, 28(27–28), 3138–3160. <https://doi.org/10.1016/j.quascirev.2009.08.016>
- Newall, J. C. H., Dymova, T., Blomdin, R., Fredin, O., Glasser, N. F., Suganuma, Y., Harbor, J. M., & Stroeven, A. P. (2020). The glacial geomorphology of western Dronning Maud Land, Antarctica. *Journal of Maps*, 16(2), 468–478. <https://doi.org/10.1080/17445647.2020.1761464>
- Nývlt, D., Braucher, R., Engel, Z., Mlčoch, B., & team, A. S. T. E. R. (2014). Timing of the northern Prince Gustav Ice Stream retreat and the deglaciation of northern James Ross Island, Antarctic Peninsula during the last glacial–interglacial transition. *Quaternary Research*, 82(2), 441–449. <https://doi.org/10.1016/j.yqres.2014.05.003>
- Nývlt, D., Fišáková, M. N., Barták, M., Stachoň, Z., Pavel, V., Mlčoch, B., & Láska, K. (2016). Death age, seasonality, taphonomy and colonization of seal carcasses from Ulu Peninsula, James Ross Island, Antarctic Peninsula. *Antarctic Science*, 28(1), 3–16. <https://doi.org/10.1017/S095410201500036X>
- Nývlt, D., Košler, J., Mlčoch, B., Mixa, P., Lisá, L., Bubík, M., & Hendriks, B. W. H. (2011). The Mendel Formation: Evidence for Late Miocene climatic cyclicity at the northern tip of the Antarctic peninsula. *Palaeogeography, Palaeoclimatology, Palaeoecology*, 299(1–2), 363–384. <https://doi.org/10.1016/j.palaeo.2010.11.017>
- Obu, J., Westermann, S., Vieira, G., Abramov, A., Balks, M. R., Bartsch, A., Hrbáček, F., Käab, A., & Ramos, M. (2020). Pan-Antarctic map of near-surface permafrost temperatures at 1 km² scale. *The Cryosphere*, 14(2), 497–519. <https://doi.org/10.5194/tc-14-497-2020>
- Oliva, M., Navarro, F., Hrbáček, F., Hernández, A., Nývlt, D., Pereira, P., Ruiz-Fernández, J., & Trigo, R. (2017). Recent regional climate cooling on the Antarctic Peninsula and associated impacts on the cryosphere. *Science of the Total Environment*, 580, 210–223. <https://doi.org/10.1016/j.scitotenv.2016.12.030>
- Pirrie, D., Crame, J. A., Riding, J. B., Butcher, A. R., & Taylor, P. D. (1997). Miocene glaciomarine sedimentation in the northern Antarctic Peninsula region: The stratigraphy and sedimentology of the Hobbs Glacier Formation, James Ross Island. *Geological Magazine*, 134(6), 745–762. <https://doi.org/10.1017/S0016756897007796>
- Píšková, A., Roman, M., Bulínová, M., Pokorný, M., Sanderson, D., Cresswell, A., Liro, J. M., Coria, S. H., Nedbalová, L., Lami, A., Musazzi, S., Van de Vijver, B., Nývlt, D., & Kapalová, K. (2019). Late-Holocene palaeoenvironmental changes at Lake Esmeralda (Vega Island, Antarctic Peninsula) based on a multi-proxy analysis of laminated lake sediment. *The Holocene*, 29(7), 1155–1175. <https://doi.org/10.1177/0959683619838033>
- Pritchard, H. D., Ligtenberg, S. R. M., Fricker, H. A., Vaughan, D. G., van den Broeke, M. R., & Padman, L. (2012). Antarctic ice-sheet loss driven by basal melting of ice shelves. *Nature*, 484(7395), 502–505. <https://doi.org/10.1038/nature10968>
- Pudsey, C. J., Murray, J. W., Appleby, P., & Evans, J. (2006). Ice shelf history from petrographic and foraminiferal evidence, northeast Antarctic Peninsula. *Quaternary Science Reviews*, 25(17–18), 2357–2379. <https://doi.org/10.1016/j.quascirev.2006.01.029>
- Rabassa, J. (1983). Stratigraphy of the glacial deposits in northern James Ross Island, Antarctic Peninsula. *INQUA Symposium on the Genesis and Lithology of Quaternary Deposits*, 329–339.
- Rabassa, J., Skvarca, P., Bertani, L., & Mazzoni, E. (1982). Glacier inventory of James Ross and Vega islands, Antarctic Peninsula. *Annals of Glaciology*, 3, 260–264. <https://doi.org/10.3189/S0260305500002883>
- Roberts, S. J., Hodgson, D. A., Sterken, M., Whitehouse, P. L., Verleyen, E., Vyverman, W., Sabbe, K., Balbo, A., Bentley, M. J., & Moreton, S. G. (2011). Geological constraints on glacio-isostatic adjustment models of relative sea-level change during deglaciation of Prince Gustav Channel, Antarctic Peninsula. *Quaternary Science Reviews*, 30(25–26), 3603–3617. <https://doi.org/10.1016/j.quascirev.2011.09.009>
- Roman, M., Nedbalová, L., Kohler, T. J., Lirio, J. M., Coria, S. H., Kopáček, J., Vignoni, P. A., Kopalová, K., Lecomte, K. L., Elster, J., & Nývlt, D. (2019). Lacustrine systems of Clearwater Mesa (James Ross Island, north-eastern Antarctic Peninsula): Geomorphological setting and limnological characterization. *Antarctic Science*, 31(4), 169–188. <https://doi.org/10.1017/S0954102019000178>
- Ruiz-Fernández, J., Oliva, M., Nývlt, D., Cannone, N., García-Hernández, C., Guglielmin, M., Hrbáček, F., Roman, M., Fernández, S., López-Martínez, J., & Antoniades, D. (2019). Patterns of spatio-temporal paraglacial response in the Antarctic Peninsula region and associated ecological implications. *Earth-Science Reviews*, 192, 379–402. <https://doi.org/10.1016/j.earscirev.2019.03.014>
- SCAR Composite Gazetteer of Antarctica. (2014). *Scientific Committee on Antarctic Research*. GCMD Metadata. http://gcmd.nasa.gov/records/SCAR_Gazetteer.html
- Seehaus, T., Cook, A. J., Silva, A. B., & Braun, M. (2018). Changes in glacier dynamics in the northern Antarctic Peninsula since 1985. *The Cryosphere*, 12(2), 577–594. <https://doi.org/10.5194/tc-12-577-2018>
- Siebert, M., Atkinson, A., Banwell, A., Brandon, M., Convey, P., Davies, B., Downie, R., Edwards, T., Hubbard, B., Marshall, G., Rogelj, J., Rumble, J., Stroeve, J., & Vaughan, D. (2019). The Antarctic Peninsula under a 1.5°C global warming scenario. *Frontiers in Environmental Science*, 7, 102. <https://doi.org/10.3389/fenvs.2019.00102>
- Smellie, J. L. (1999). Lithostratigraphy of Miocene-recent, alkaline volcanic fields in the Antarctic Peninsula and

- eastern Ellsworth Land. *Antarctic Science*, 11(3), 362–378. <https://doi.org/10.1017/S0954102099000450>
- Smellie, J. L. (2006). The relative importance of supraglacial versus subglacial meltwater escape in basaltic subglacial tuya eruptions: An important unresolved conundrum. *Earth-Science Reviews*, 74(3-4), 241–268. <https://doi.org/10.1016/j.earscirev.2005.09.004>
- Smellie, J. L., Johnson, J. S., McIntosh, W. C., Esser, R., Gudmundsson, M. T., Hambrey, M. J., & van Wyk de Vries, B. (2008). Six million years of glacial history recorded in volcanic lithofacies of the James Ross Island Volcanic Group, Antarctic Peninsula. *Palaeogeography, Palaeoclimatology, Palaeoecology*, 260(1-2), 122–148. <https://doi.org/10.1016/j.palaeo.2007.08.011>
- Smellie, J. L., Johnson, J. S., & Nelson, A. E. (2013). *Geological map of James Ross Island. 1. James Ross Island Volcanic Group. BAS GEOMAP 2 series, sheet 5, 1:125 000*. British Antarctic Survey.
- Sterken, M., Roberts, S. J., Hodgson, D. A., Vyverman, W., Balbo, A. L., Sabbe, K., Moreton, S. G., & Verleyen, E. (2012). Holocene glacial and climate history of Prince Gustav Channel, northeastern Antarctic Peninsula. *Quaternary Science Reviews*, 31, 93–111. <https://doi.org/10.1016/j.quascirev.2011.10.017>
- Strelin, J. A., & Malagnino, E. C. (1992). *Geomorfología de la Isla James Ross. Geología de la Isla James Ross*. 7-36. Instituto Antártico Argentino.
- Strelin, J. A., Sone, T., Mori, J., Torielli, C. A., & Nakamura, E. (2006). New data related to Holocene landform development and climatic change from James Ross Island, Antarctic Peninsula. In D. K. Fütterer, D. Damaske, G. Kleinschmidt, H. Miller, & F. Tessensohn (Eds.), *Antarctica: Contributions to Global Earth sciences. Proceedings of the IX International Symposium of Antarctic Earth Sciences, Potsdam, 2003* (pp. 455–460). Springer.
- Turner, J., Colwell, S. R., Marshall, G. J., Lochlan-Cope, T. A., Carelton, A. M., Jones, P. D., Lagun, V., Reid, P. A., & Logovkina, S. (2005). Antarctic climate change during the last 50 years. *International Journal of Climatology*, 25(3), 279–294. <https://doi.org/10.1002/joc.1130>
- Turner, J., Lu, H., White, I., King, J. C., Phillips, T., Scott Hosking, J., Bracegirdle, T. J., Marshall, G. J., Mulvaney, R., & Deb, P. (2016). Absence of 21st century warming on Antarctic Peninsula consistent with natural variability. *Nature*, 535(7612), 411–415. <https://doi.org/10.1038/nature18645>
- van Lipzig, N. P. M., King, J. C., Lachlan-Cope, T. A., & van den Broeke, M. R. (2004). Precipitation, sublimation, and snow drift in the Antarctic Peninsula region from a regional atmospheric model. *Journal of Geophysical Research*, 109(D24), D24106. <https://doi.org/10.1029/2004JD004701>
- Vaughan, D. G., Marshall, G. J., Connelly, W. M., Parkinson, C., Mulvaney, R., Hodgson, D. A., King, J. C., Pudsey, C. J., & Turner, J. (2003). Recent rapid regional climate warming on the Antarctic Peninsula. *Climatic Change*, 60(3), 243–274. <https://doi.org/10.1023/A:1026021217991>
- Watcham, E. P., Bentley, M. J., Hodgson, D. A., Roberts, S. J., Fretwell, P. T., Lloyd, J. M., Larter, R. D., Whitehouse, P. L., Leng, M. J., Monien, P., & Moreton, S. G. (2011). A new Holocene relative sea level curve for the South Shetland Islands, Antarctica. *Quaternary Science Reviews*, 30(21-22), 3152–3170. <https://doi.org/10.1016/j.quascirev.2011.07.021>
- Yildirim, C. (2020). Geomorphology of Horseshoe Island, Marguerite Bay, Antarctica. *Journal of Maps*, 16(2), 56–67. <https://doi.org/10.1080/17445647.2019.1692700>